J Electroceram (2010) 24:1–4
DOI 10.1007/s10832-007-9360-7

Fabrication, property and application of novel pyroelectric single crystals—PMN–PT

Ping Yu · Yanxue Tang · Haosu Luo

Received: 30 September 2007 / Accepted: 6 November 2007 / Published online: 20 November 2007

Abstract The pyroelectric properties and temperature stability of $Pb(Mg_{1/3}Nb_{2/3})O_3$–$xPbTiO_3$(PMN–xPT) single crystals ($0.13 \leq x \leq 0.40$) were investigated. The best choice for pyroelectric performance is [111]-oriented PMN–0.26PT single crystal whose figures of merit for voltage responsivity and detectivity are 0.11 m^2/C and 15×10^{-5} $Pa^{-1/2}$, respectively. However, the [001]-oriented PMN–0.37PT single crystal has much better temperature stability, whose temperature coefficient of pyroelectric property is 0.5%/K in the range of 20 °C to 55 °C, and Curie temperature is high: 175 °C. We also found that PMN–xPT possessed low thermal diffusivity $D\sim4.4\times10^{-7}$ m^2/s, low volume specific heat $C_v\sim2.5\times10^6$ J/m^3 K and tunable permittivity $\varepsilon\sim$(300–7000). The pyroelectric performances of PMN–xPT single crystals are superior to those of conventional pyroelectric materials and promising for IR device applications.

Keywords Pyroelectric detector · PMN–xPT · FOMs

1 Introduction

Pyroelectric infrared detectors have been of-interest and studied for many years because of their wide wavelength response, lack of need for cooling, high stability, high sensitivity and also their very low cost [1]. The single (or dual) element pyroelectric detectors are widely used in body detectors, flame and fire detectors, IR spectrometry, and gas analyzers. Recent years, more attentions are focused on the arrays of pyroelectric elements, and they have a variety of applications such as thermal imaging and infrared camera [2].

Relaxor-based ferroelectric $Pb(Mg_{1/3}Nb_{2/3})O_3$–$xPbTiO_3$ (PMN–xPT) single crystals are very excellent as piezoelectric and electro-optic materials [3–7]. Recently, we have also found that PMN–xPT crystals exhibit high pyroelectric effects [8]. Compared to conventional pyroelectric bulk ceramics or thin films, single crystals offer many advantages, such as homogeneity, compositional and microstructural controllability. We investigated the properties of these pyroelectric single crystals by three major figures of merit (FOMs): current responsivity $F_i = p/C_v$, voltage responsivity $F_v = p/(C_v\varepsilon_0\varepsilon_r)$, and detectivity $F_d = p/\left[C_v(\varepsilon_0\varepsilon_r \tan\delta)^{1/2}\right]$ [2], where p, C_v, ε_0, ε_r, and $\tan\delta$ are the pyroelectric coefficient, volume specific heat, permittivity of free space, relative dielectric constant and dielectric loss, respectively. In general, it is the higher FOMs, and the higher pyroelectric coefficient, lower dielectric constant and loss. For practical applications, it is also very important to know the temperature coefficient of these pyroelectric performances. It affects the detector stability due to the change of pyroelectric and dielectric performances.

At room temperature, the structures of PMN–xPT single crystals are rhombohedral (R) for $x \leq 0.3$ and tetragonal (T) for $x \geq 0.35$, with spontaneous polarization along the <111> and <001> direction, respectively [9]. The R–T morphotropic phase boundary (MPB) is in the range $0.30 < x < 0.35$. The PT concentration (x) was determined by using the dielectric maximum temperature (T_m) obtained upon heating (zero field heating), i.e., estimated by $x\times100=[T_m(°C)+10]/5$ [10]. In general, the pyroelectric coefficient oriented along the spontaneous polarization direction is larger than that of oriented other directions [11]. So the poling direction of PMN–xPT for pyroelectric application is along the sponta-

P. Yu (✉) · Y. Tang · H. Luo
Shanghai institute of Ceramics, Chinese Academy of Sciences, Shanghai 201800, China
e-mail: yuping2210@mail.sic.ac.cn

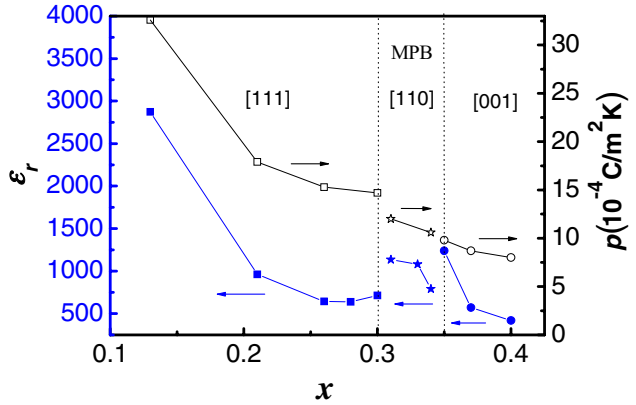

Fig. 1 Composition dependence of permittivity at 1 kHz and pyroelectric coefficient of PMN–*x*PT single crystals at room temperature

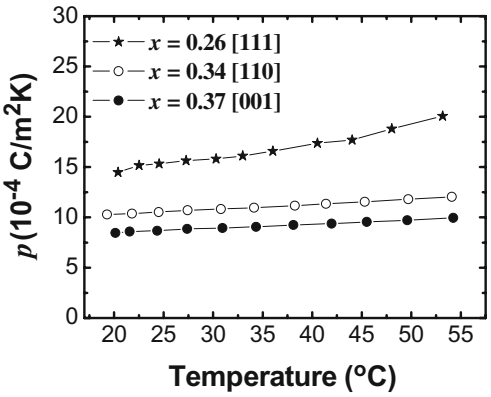

Fig. 2 Pyroelectric coefficient as a function of temperature for [111]-oriented PMN–0.26PT, [110]-oriented PMN–0.34PT and [001]-oriented PMN–0.38PT single crystals

neous polarization, which is different from the cases for piezoelectric applications.

The purpose of this paper is to present a systematic investigation of the pyroelectric performances of PMN–*x*PT single crystals and the principles of selection for different requirements of processing and devices.

2 Experiment

PMN–*x*PT single crystals were grown by a modified Bridgman technique [12]. The as-grown PMN–*x*PT crystals were oriented using an X-ray diffractometer and cut into rectangular shaped specimens around 5×5×0.3 mm^3. The samples were coated with silver electrode and poled under an electric field of 1 kV/mm for 15 min near below their T_c in silicone oil, and then slowly cooled to room temperature while maintaining half of the applied electric field.

The pyroelectric coefficients were measured by a dynamic technique [13] using sinusoidal temperature change with amplitude of 1 °C at a frequency of 45 mHz. The dielectric properties were measured by a HP4194A impedance analyzer. Piezoelectric coefficient (d_{33}) was measured using a Berlincourt-type quasistatic d_{33} meter at a frequency of 55 Hz.

3 Results and discussion

3.1 Pyroelectric properties

The pyroelectric coefficient (p) is described as a vector giving the rate of change of the spontaneous polarization (P_s) with temperature (T). Figure 1 shows the value of both p and ε_r (1 kHz) as a function of x for [111]-, [110]-, and [001]-oriented poled PMN–*x*PT single crystals at room temperature. The largest value of p is 32.6×10^{-4} C/m^2 K for PMN–0.13PT and decrease with the increasing compositions of $PbTiO_3$. The remnant polarization (P_r) of PMN–*x*PT single crystals along spontaneous polarization direction at room temperature does not vary a lot over the composition range $0.13 \le x \le 0.40$. The decreases in pyroelectric coefficients are attributed to the composition variations that shift T_c significantly from ~ 55 °C to ~ 190 °C, and thus make P_r decreases towards zero over a wider temperature range with increasing x.

Table 1 Summary of property parameters of PMN–*x*PT single crystals for pyroelectric devices at room temperature.

PMN–*x*PT	T_C (°C)	Trt/Td (°C)	p (10^{-4} C/m^2 K)	ε_r (1 k Hz)	tanδ (1 k Hz)	F_i (10^{-10}m/V)	F_v (m^2/C)	F_d (10^{-5} Pa$^{-1/2}$)
0.13	58	–	32.6	3107	0.0034	13.0	0.046	13.5
0.21	95	–	17.9	961	0.003	7.2	0.08	14.2
0.26	121	92	15.3	643	0.0028	6.1	0.11	15.3
0.30	140	92	14.7	714	0.0031	5.9	0.09	13.3
0.31	146	89	12.0	1136	0.004	4.8	0.05	7.6
0.34	158	75	10.6	790	0.005	4.2	0.06	7.2
0.35	162	12	9.8	1238	0.0054	3.9	0.04	5.1
0.37	173	−5	8.7	570	0.0041	3.5	0.07	7.6
0.40	191	<−150	8.0	420	0.005	3.2	0.09	7.4
$LiTaO_3$	620	–	1.6	42	0.0005	0.5	0.13	11.5
TGS	49	–	3.5	33	0.005	1.4	0.42	11.6

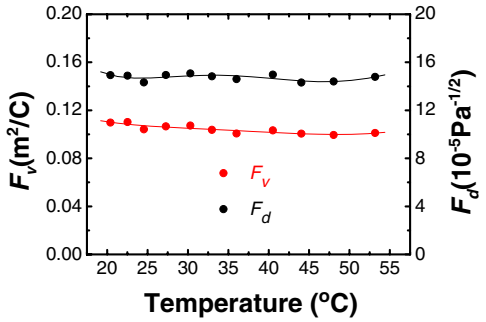

Fig. 3 Figures of merit F_v and F_d as a function of temperature for [111] oriented PMN–0.26PT single crystal

Fig. 5 The pyroelectric detectors with single element

The permittivity is lower when the specimens are poled along their spontaneous polarization directions (Fig. 1), where the domain structures of these poled crystals are more similar to monodomain structures. The role of domain wall which contribute to the permittivity could be weaker. The dielectric loss of these specimens is mostly lower than 0.005 (Table 1), which is an advantage to achieve high F_d.

3.2 Temperature stability

The pyroelectric coefficient of these materials actually increases when increasing the temperature up to the Curie point. This characteristic will manifest itself as detector temperature "drift". Figure 2 shows the pyroelectric coefficient as a function of temperature for different compositions of PMN–xPT single crystals. the value of p for [111] oriented rhombohedral PMN–0.26PT single crystal increases from 14.5×10^{-4} to 20.6×10^{-4} C/m^2 K with temperature increasing from 20 °C to 55 °C. For [110]-oriented orthorhombic PMN–0.34PT, and [001]-oriented tetragonal PMN–0.37PT single crystals, the pyroelectric coefficient is nearly independent of temperature over the temperature range. The temperature coefficients of the three typical compositions are 1.2%/K, 0.5%/K and 0.5%/K, respectively. The temperature coefficient affects the performance of IR devices if the short circuit mode is applied, but it will be overlaid by the changing of permittivity with the temperature using the open-circuit-operation. The weak temperature dependence of F_v and F_d (both have the factors p and ε_r) for PMN–xPT is shown in Fig. 3.

For PMN–0.26PT, a dielectric shoulder near 100 °C occurred, which may be caused by the transition from macrodomain to microdomain states. A diffuse ferroelectric phase transition occurs near 120 °C between ferroelectric and paraelectric state. For PMN–0.37PT, a nearly normal ferroelectric phase transition takes place at 175 °C (Fig. 4). During the process of cutting, thinning and polishing of the crystals, and the deposition of electrode and gold–black on the thin detection elements, the temperature of the crystals should be below the transition temperature in order to avoid depoling. Depoling effect will decrease the remnant polarization dramatically and induce the decline of pyroelectric properties. Large pyroelectric response of PMN–xPT maintains in a broad range for temperature below 70 °C, and the temperature range for tetragonal PMN–xPT ($x\geq0.35$) is higher.

Further more, low C_v is most desirable for high FOMs, and low D is vital to obtain high-temperature resolution for pyroelectric devices. Take [111]-oriented PMN–0.26PT for example, $C_v\sim2.5\times10^6$ J/m^3 K, $D\sim4.4\times10^{-7}$ m^2/s. They are lower than those of $LiTaO_3$ ($C_v\sim3.2\times10^6$ J/m^3 K, $D\sim13\times10^{-7}$ m^2/s). Because all pyroelectric detectors are used in a high vibration or acoustically noisy environment, piezoelectric properties are also important in pyroelectric devices, which will produce a piezoelectric microphonic noise signal. The selection of a low piezoelectric coefficient

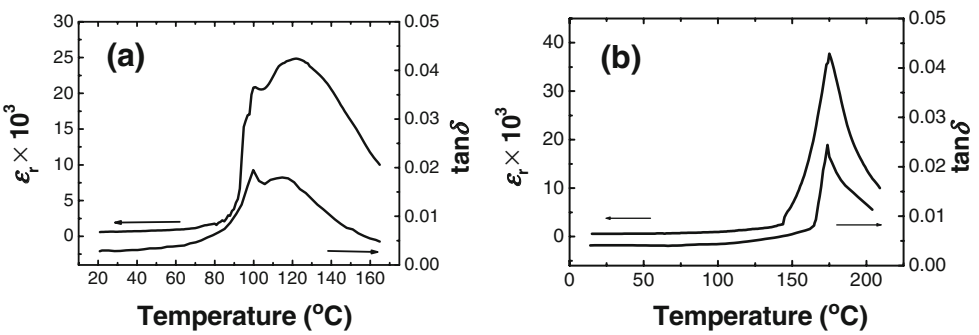

Fig. 4 Dielectric characteristics at 1 kHz for (**a**) [111]-oriented PMN–0.26PT and (**b**) [001]-oriented PMN–0.37PT single crystal as a function of temperature

material could be a valuable consideration. The piezoelectric coefficients (d_{33}) of rhombohedral and tetragonal PMN–xPT single crystals are around 100pC/N and 250pC/N, respectively, and d_{31} of rhombohedral PMN–xPT is around −90pC/N. The d_{33} and d_{31} of PMN–xPT along the spontaneous polarization direction are small [14]. Many methods can reduce the microphonic noise [15], and in this work, we placed the detector in a rigid package. The sensitive element which coated with electrodes, in the middle of the specimen, was clamped by the other area around it (see Fig. 5), which can reduce the d_{31}. Compensated detector structure is also useful to minimize the piezoelectric effect. Table 1 summarizes the pyroelectric properties and figures of merit of PMN–xPT single crystals as a function of x, and it also compares these values of conventional pyroelectric materials.

3.3 Prototype of device

Some attempt work on pyroelectric device of PMN–xPT single crystals has been done. Figure 5 shows the single element pyroelectric detector and the interior view of it. The element size is Φ2 mm PMN–0.26PT with metal black layer. The thickness is 60 μm and the electrodes are NiCr. The detector was irradiated by chopped infrared radiation from a blackbody furnace at 500 K, and the frequency is 12.5 Hz. The results of voltage responsivity and detectivity are 211 V/W and $D^*(500, 12.5,1)=1.06\times10^8$ cm $Hz^{1/2}$ W^{-1}, respectively. The performance already has met the requirement of the practical device, although the prototype can be improved greatly through optimizing the device structure design, improving the processing of the single crystals and decreasing the thickness of the elements.

4 Conclusion

In summary, large pyroelectric coefficients were observed in the PMN–xPT single crystals. The optimum single crystals for pyroelectric applications were found to be [111]-oriented rhombohedral PMN–xPT ($0.21\leq\times\leq0.30$) which is provided with high pyroelectric coefficients and FOMs. The optimum one for temperature stability was found to be [001]-oriented tetragonal PMN–xPT ($0.35\leq\times\leq0.40$) with high T_c and it is also easy to process. Near the room temperature, the pyroelectric properties of PMN–xPT are weakly temperature dependent. Consequently, PMN–xPT single crystals offer outstanding performances and are promising candidates for high-performance infrared detectors and imager applications.

Acknowledgments This work was supported by the 863 High Technology and Development Project of the People's Republic of China (Grant No. 2006AA03Z107), CAS Innovation Program (QJ14), the Natural Science Foundation of China (50432030 and 50602047), Shanghai Municipal Government (05JC14079 and 06DZ05116), Innovation Funds from Shanghai Institute of Ceramics of Chinese Academy of Science (SCX0608), and Dr. Jinglan Sun from Shanghai institute of technical physics, Chinese academy of sciences.

References

1. R.W. Whatmore, J. Electroceram. **13**, 139 (2004)
2. R.W. Whatmore, Rep. Prog. Phys. **49**, 1335 (1986)
3. R.F. Service, Science. **275**, 1878 (1997)
4. Z. Yin, H. Luo, P. Wang, G. Xu, Ferroelectrics. **299**, 207 (1999)
5. S.-E. Park, T.R. Shrout, J. Appl. Phys. **82**, 1804 (1997)
6. X. Wan, H.L.W. Chan, C.L. Choy, X. Zhao, H. Luo, J. Appl. Phys **96**, 1387 (2004)
7. X. Wan, H. Luo, J. Wang, H.L.W. Chan, C.L. Choy, Solid State Commun. **129**, 401 (2004)
8. Y. Tang, X. Zhao, X. Feng, W. Jin, H. Luo, Appl. Phys. Lett. **86**, 082901 (2005)
9. A.K. Singh, D. Pandey, J. Phys. Condens. Matter **13**, 931 (2001)
10. Z. Feng, H. Luo, Y. Guo, T. He, H. Xu, Solid State Commun. **126**, 347 (2003)
11. M. Davis, D. Damjanovic, N. Setter, J. Appl. Phys. **96**, 2811 (2004)
12. H.S. Luo, G.H. Xu, H.Q. Xu, P.C. Wang, Z.W. Yin, Jpn. J. Appl. Phys. **39**, 5581 (2000)
13. V. Fuflyigin, E. Salley, A. Osinsky, P. Norris, Appl. Phys. Lett. **77**, 3075 (2000)
14. R. Zhang, B. Jiang, W. Cao, Appl. Phys. Lett **82**, 787 (2003)
15. N.M. Shorrocks, R.W. Whatmore, M.K. Robinson, S.G. Porter, Proc. SPIE **588**, 44–51 (1985)